MAPPING THE EXCAVATION DISTURBED ZONE AROUND THE MINE-BY TUNNEL USING INDUCED SEISMICITY AND VELOCITY IMAGING

S.C. MAXWELL, R.P. YOUNG, C. BAKER, and D.S. COLLINS
Keele University Applied Seismology and Rock Physics Laboratory, U.K.
C.D. MARTIN
GRC, Laurentian University, Sudbury, Ont., Canada.

ABSTRACT

The potential for mapping the EDZ using a combination of induced seismicity and velocity imaging is presented using the Mine-by tunnel as a specific case study. Concentrations of induced seismic events have been used to locate regions of induced fracturing, as well as changes in location with time to monitor progressive failure. Estimates of the size, magnitude and stress release during the events can also be used to assess the nature of the seismic deformation. In particular, moment tensor inversions are employed to examine the micro-mechanics of the seismic deformation. Images of the rock mass velocity structure around the tunnel are also used with the seismicity to investigate the rock mass response to excavation-induced stress changes. The Mine-by experiment thereby serves as a comprehensive example of applying seismological techniques in EDZ investigations.

INTRODUCTION

One component of the excavation disturbance zone (EDZ) investigation in AECL's Mine-by experiment [1] was the use of induced microseismicity as a characterization tool. At a depth of 420 m below surface, the 3.5 m diameter Mine-by tunnel through homogenous, unfractured granite was excavated using rock breaking methods. A comprehensive suite of geomechanical instrumentation, including extensometers and stress cells, was emplaced to validate numerical simulation of the rock mass deformation adjacent to the excavation [1]. After excavation began, breakout notches formed in the roof and floor of the tunnel. The notch was formed orthogonal to the maximum principal stress direction, and is analogous to borehole overbreak commonly observed around deep boreholes. A high frequency (up to 10 kHz) array [2], consisting of 16 triaxial accelerometers was installed to monitor seismicity induced by the excavation (Figure 1). A catalog of 25,000 microearthquake/acoustic emissions (magnitude < 0) were recorded between September, 1991 and August, 1992. These microearthquakes correspond to the induced fracturing in the EDZ as the rock mass responds to changes in the stress field around the tunnel, although vibrations during the passage of the

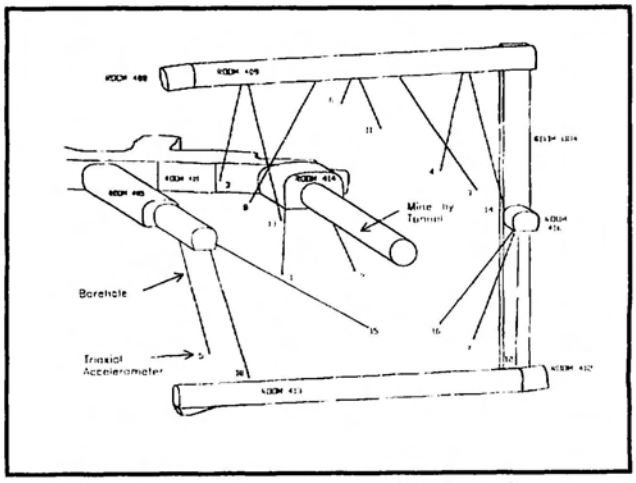

Figure 1. Perspective view of the tunnel.

associated dynamic waves does not result in any secondary damage.

This paper describes the seismological analysis of these events and the relation to the EDZ. The relationship between the EDZ and the 3D seismic velocity structure around the tunnel computed with data from the seismic array of both small blasts and induced microseismicity will also be described. Finally, the potential role of seismological techniques in a comprehensive geomechanical programme will be discussed.

INDUCED SEISMICITY

The most basic seismic parameter is the hypocentral location of the microearthquake. Generally, the induced seismicity was concentrated immediately above and below the tunnel in the vicinity of the notches (Figure 2). The location accuracy of the induced seismicity was measured using small calibration blasts, which indicated an average location uncertainty of roughly ±.25 m [2]. The seismicity is attributed to the rock mass fracturing associated with the notch formation, so that the locations can be used to delineate the actively deforming regions. The numbers of events in a particular area can also be used as a simplistic estimate of the degree of damage, as illustrated in Figure 2, where the maximum concentration corresponds with the fractured rock in the notch region. Another way in which the seismicity can be used to assess the EDZ is to examine spatial and temporal changes in the locations. For example, Figure 3 shows the locations of microseismic events located in the upper notch region in a central 1 m axial segment of the tunnel, for three different time periods [3]. Between the first two time periods, the tunnel face has moved from immediately at the segment to a point 1.5 m away. During this period, the events can be seen to migrate into the rock mass away from the edge of the tunnel. In the next interval, the tunnel face moves an additional 3 m and the events are seen to shift further away from the tunnel. These spatial shifts in the seismically active regions, are attributed to progressive failure extending further into the rockmass with time, and can be visually correlated with the notch development.

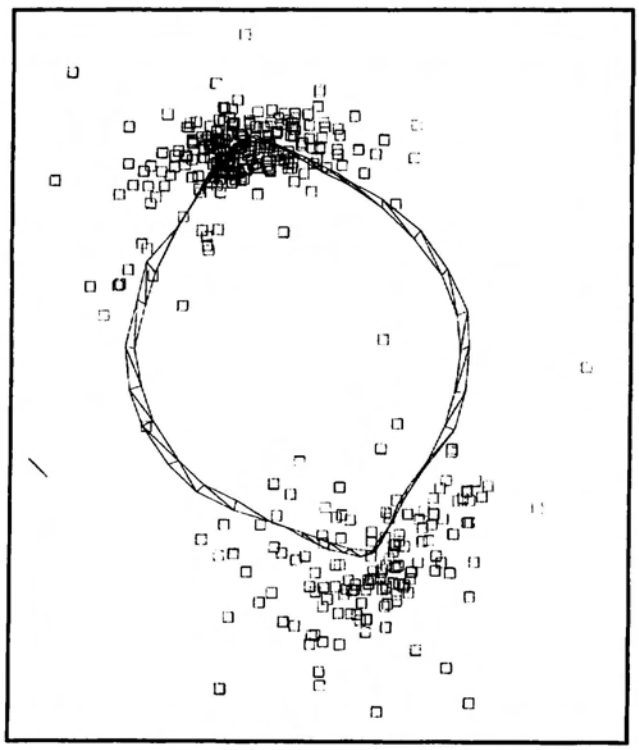

Figure 2. Axial view of the tunnel (3.5 m original diameter) showing the induced seismicity.

Source parameters were also computed for the microearthquakes, to estimate the seismic magnitude, stress release, energy release and area of the coseismic deformation assuming a shear failure model [4]. In Figure 3, the symbols are scaled to source radius which is a measure of the area of deformation. Using standard earthquake models, the source radius is computed assuming instantaneous, homogeneous shear failure over a circular fault [5]. Clearly, this represents a simplistic model of the real deformation, where deformation is probably restricted to a relatively

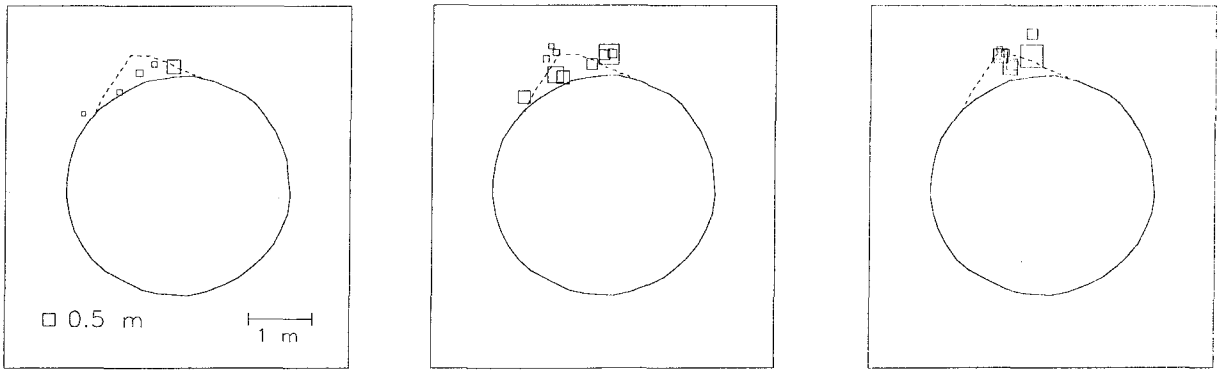

Figure 3. Induced seismicity located within the central 1 m segment of the tunnel, during three time periods. Symbols are scaled to the source radius of the seismic deformation.

small region. Although, the source radius will therefore be overestimated, the relative trends in area of deformation can be investigated. Generally, the events furthest from the tunnel tend to have relatively small source radii. These regions would correspond to fracture initiation, where the seismic deformation occurs over a relatively small zone. With time, these fractures will tend to coalesce so that further seismic deformation can occur over a relatively larger area. Through this combined interpretation of the location and source parameters of the microearthquakes, seismic deformation associated with fracture initiation and reactivation of failure on previously created fractures can be distinguished.

Seismic moment, a measure of the size of the microearthquake, was also computed [5]. Figure 4 shows the moments of the events from the central portion of the tunnel, plotted against the axial location relative to the tunnel face position at the time of each event. The largest events are found in the vicinity of the face, with relatively smaller events ahead of the face associated with pre-fracturing of the rock mass prior to the tunnel excavation. Small events also occur behind the tunnel face, in the notch regions. Similar trends can be seen in plots of the coseismic stress release.

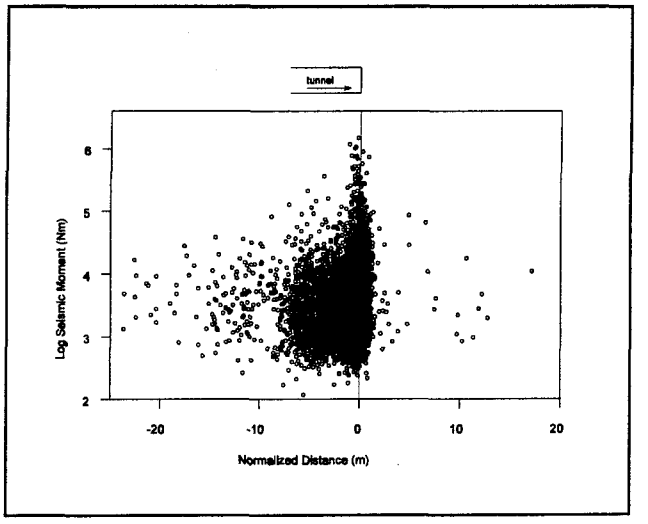

Figure 4. Seismic moment versus axial location relative to the tunnel face.

In order to examine the forces acting during the seismic failure, moment tensor (MT) analysis techniques have been used [6]. These techniques allow the determination of information about the source by examining the characteristics of the recorded seismograms. Moment tensor

results may be used to investigate the micromechanics of the fracturing by assessing the relative amounts of shear, implosional or explosional failure which occurred during the seismic deformation process. Two different approaches have been applied. Time independent MT analysis, assuming homogenous deformation during the seismic event, indicated that approximately 50% of the events include significant (>30%) non-shear components [7]. Time dependent MT analysis, where the changes in the deformation which occur during the seismic event are computed, has also been used [8]. This has the advantage that the significance of the non-shear part of the failure mechanism during the seismic event can be evaluated. For example, a series of events from the region ahead of the face from an early excavation round were analysed using a time dependent MT technique (Figure 5). The results indicate that the early events show a significant initial component of 'explosional' tensile failure (Figure 6 shows an example of one such event). This may be related to cracks opening perpendicular to the local σ_3 direction. The latter part of the failure mechanism occurs by a predominantly shear-type mechanism. Later events show shear mechanisms throughout their rupture history. The small group of events which show an implosional onset are associated with the borehole collapse during excavation and are not directly associated with the EDZ.

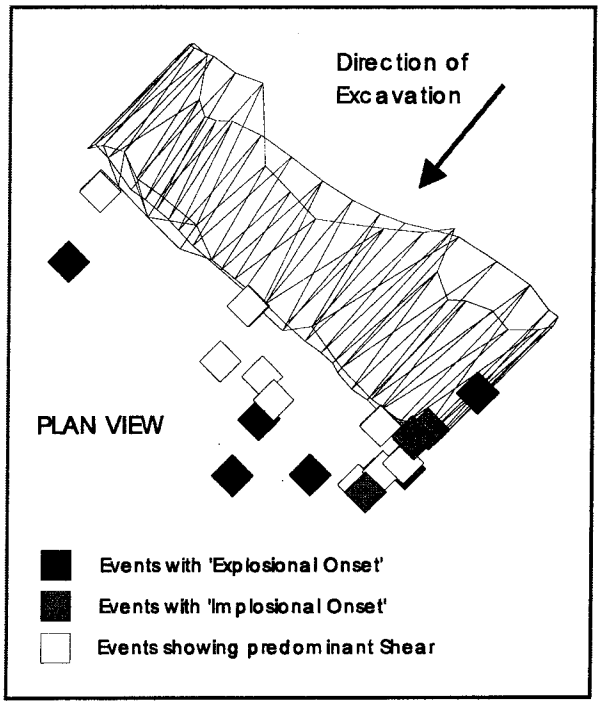

Figure 5. Initial failure mechanisms of events from an early excavation round.

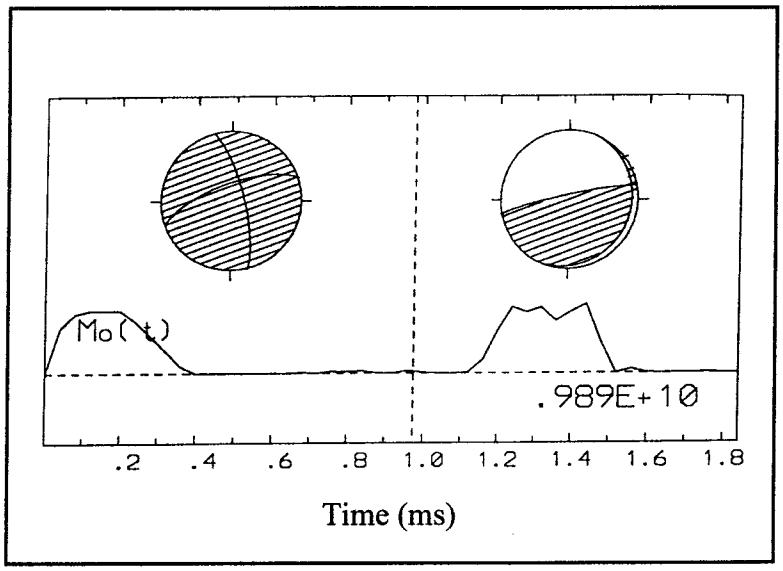

Figure 6. Example of a temporal change in failure mechanism from 'explosive' to shear during the seismic event.

VELOCITY STRUCTURE

In order to calibrate the in-situ velocity structure and to assess the accuracy of the source locations, a series of controlled seismic sources were recorded with the microseismic array. A series of blasting caps were detonated in short holes down the length of a horizontal test tunnel, and p-wave travel times to the microseismic sensors were measured [9]. The travel times were then inverted to image the 3D velocity structure around the tunnel, by accounting for the observed anisotropy near the tunnel. Figure 7 shows the resulting velocity image plotted on a 2D cutting plane orthogonal to the tunnel axis, superimposed with the location of microseismic events located in that section of the tunnel. Velocities are plotted as relative perturbations from an initial starting model of the average velocity measured around the tunnel (lower than the intact rockmass velocity due to velocity decreases in the anisotropic slow direction). Figure 7 also shows a plot of the magnitude of the maximum compressive stress, computed using a boundary element program designed to compute elastic stress changes around underground openings (EXAMINE3D, Corkum and Curran, 1992). Generally, the velocity image shows relatively decreased values in the sidewalls of the tunnel where a tensile stress field exists. Increased velocities are seen near the high stress anomalies in the seismically active regions of the notches. The high velocity anomaly is located away from the tunnel wall, due to non-elastic fracturing associated with the notch formation. Beyond the notch region where elastic deformation is occurring, *in situ* geomechanical measurements validated elastic stress changes. The seismicity appears to be locating in a region of velocity gradient, corresponding to the region separating the plastically deformed or failed zone from the elastically, highly-stressed zone. The relatively high velocity in the highly stressed notch are due to relative closure of the microcracks, as the velocity returns to the intact rockmass velocity from the initial decreased average velocity model used in the inversion.

A prototype microvelocity logging probe was developed to validate these velocity variations [10]. The probe measures the travel time of a seismic wave between two fixed transducers, and enables fast logging of the variation in velocity down a borehole. Figure 8 shows the logging

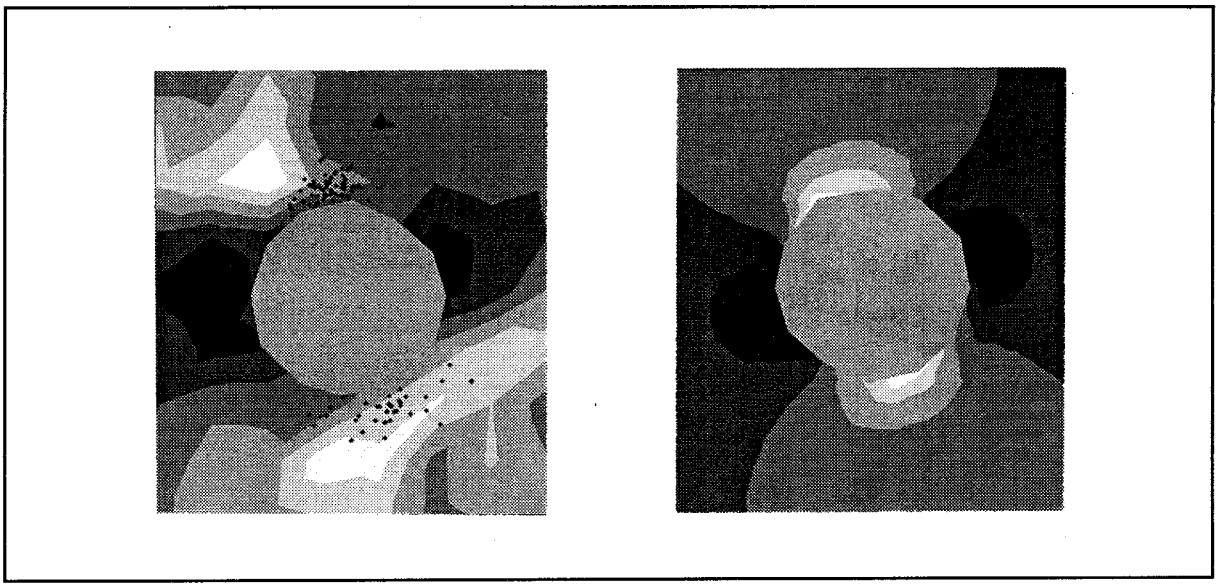

Figure 7. Contours of seismic velocity (left, -.2 to .3 km/s, dark to light) and maximum compressive stress (centre, 0 to 140 MPa) around the tunnel.

results in a horizontal radial borehole, through the low velocity region shown in Figure 7. the velocity can be seen to increase with distance away from the borehole, as the relative microcrack damage in the tensile zone decreases. Also shown is the result of logging the core from the hole, which indicates roughly a 57% decrease in velocity due to stress relief microcracking in the core during the overcoring. These results highlight the potential of assessing the EDZ using a simple geophysical tool.

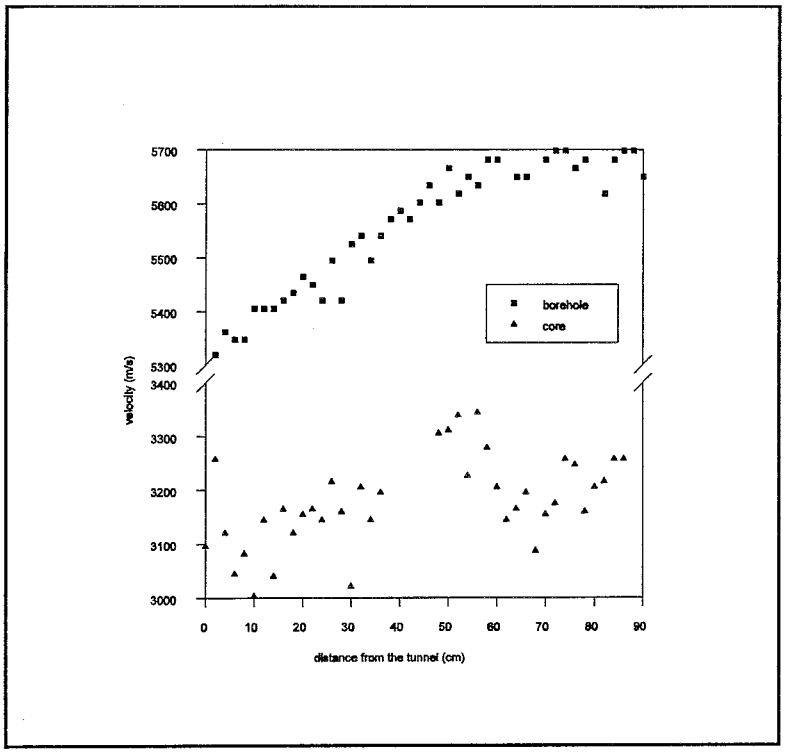

Figure 8. Borehole and core velocity logging results for a horizontal borehole in the sidewall of the tunnel.

Velocity images can also be produced using the induced earthquakes [11], which provide details of the velocity structure contemporaneous with the seismicity. The technique provides details of the velocity structure in the seismically active regions of interest. Events recorded during a three day period following the excavation of a 1 m segment of the tunnel were selected and sorted to yield the best constrained source locations recorded on a maximum number of channels [12]. A total of 60 well-located events in the upper half of the tunnel were selected. Figure 9 shows the velocity image on a plane parallel to the tunnel axis, through the centre of the notch zone. The image is superimposed with microseismic events located within 0.5 m of the plane. The image shows a low velocity region, which extends further into the rock progressively away from the tunnel face, which is mimicking the known geometry of the fractured zone. A relatively high velocity region is seen in the image, corresponding to the highly stressed, intact rock beyond

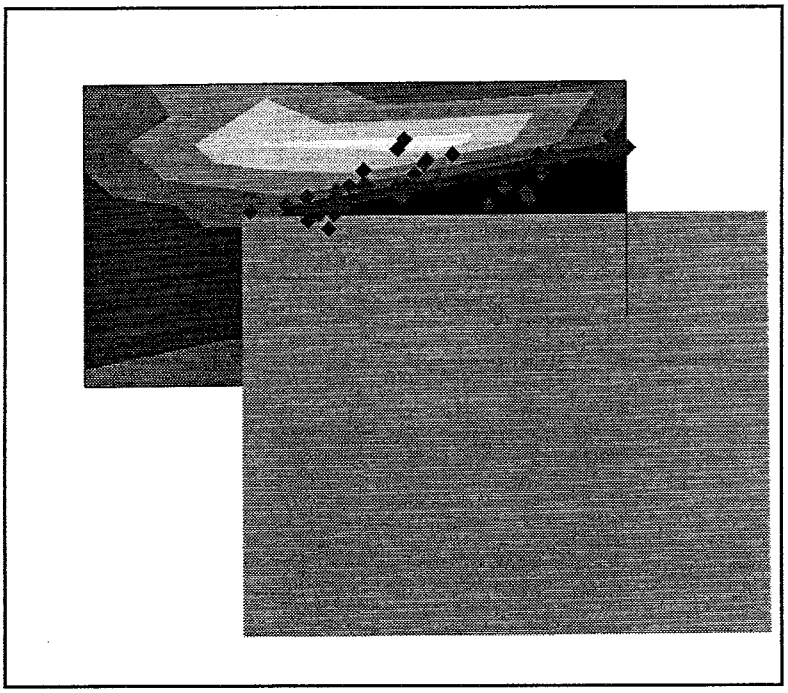

Figure 9. Side view of the tunnel with the passive-source velocity image on an axial plane (-.14 to .14 km/s) with induced seismicity.

the fractured zone. The induced seismicity is clearly located in a region of velocity transition.

DISCUSSION AND CONCLUSION

The Mine-by tunnel excavation serves as a controlled case study illustrating the potential of remotely assessing the EDZ with seismological techniques. The location of the excavation-induced seismicity can be used to evaluate the extent of the failure zone around an underground opening. Furthermore, changes in location of the induced seismicity with time can be used to monitor progressive failure. The induced seismicity appears to correspond to fracture initiation and deformation and coalescence of fractures already created. However, using seismic source parameters to characterize the size and extent of the event, it should be possible to differentiate between these two types of events. Moment tensor results can also provide details of the micromechanics of the fracturing.

Velocity imaging of the rock mass around the Mine-by tunnel was also used to map the EDZ. Velocity images were able to resolve velocity changes corresponding to the different geomechanical regimes around the tunnel. In particular, passive-source tomography was able to image the velocity structure in a specific location and point-in-time. Although the induced seismic events were all relatively low magnitude, this example serves as a simple, controlled experiment which verifies that a combination of velocity images and induced seismicity can be used to map stress changes.

One of the interesting points about this experiment is that simple 2D numerical models were unable to predict the notch prior to the excavation. The maximum stress concentration of approximately 150 MPa is significantly less than laboratory strength estimates of the intact rock [13]. This disparity has been attributed to rock mass damage ahead of the tunnel face which lowers the rock mass strength. For example, Figure 10 shows a comparison of 3D elastic estimates of the deviatoric stress in the roof of the tunnel with the number of seismic events recorded [14]. Seismic events are clustered near the tunnel face, where the deviatoric stress is rapidly changing. This suggests that the cracking initiates at stresses lower than the final stress state, including those ahead of the face. Clearly the stress path is important to the rock mass strength and therefore to the final damage. The induced seismicity and velocity information therefore offer unique observations of the location and extent of the damage during different time periods to calibrate/validate numerical models.

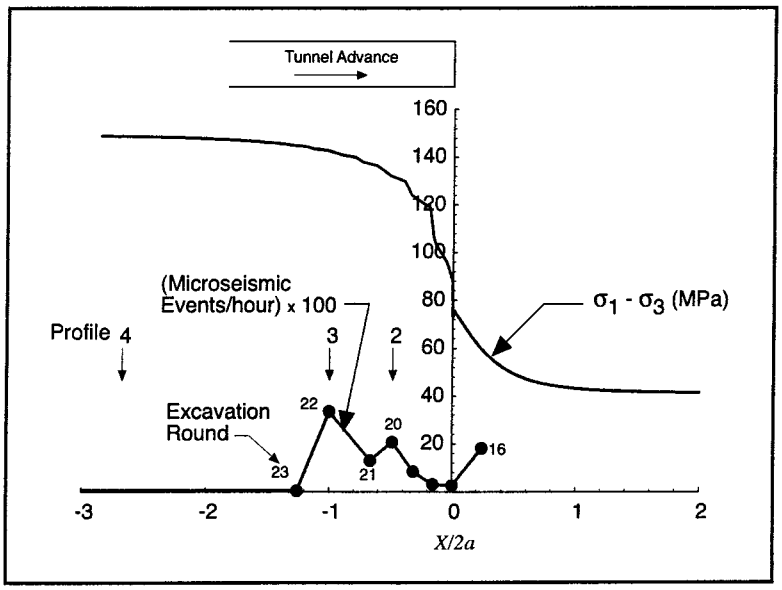

Figure 10. Comparison of the maximum deviatoric stress change in the roof of the tunnel with microseismic event rate.

The Mine-by experiment offered the possibility to record some of the highest quality microearthquakes seismograms ever recorded. This data quality was possible in part due to the careful optimization and design of the data aquisition [15], but also due to the stress state and seismic transmission properties of the rock mass. Similar results to those shown in this case study are possible at other sites (e.g. see Falls and Young, this volume), although the details of the seismic monitoring will depend heavily on the local conditions of the particular experiment. The main controlling factors will be:

1. *stress state:* At lower stress levels, the induced fracturing damage will obviously be less and so will the magnitude range and frequency content of the seismograms. Generally, lower magnitude/higher frequency events would occur at lower stresses.
2. *excavation dimensions:* The size and shape of the excavation will dictate the stress concentrations and possible size of the fractured zone, with smaller excavation having a similar effect to lower stress levels.
3. *seismic transmission:* In less competent and fractured rock masses, higher seismic attenuation will cause the progressive loss of the high frequency components of the seismogram with transmission distance. To monitor relatively high frequencies, the seismic array will have to be close to the expected seismic target zone and may have a limited area over which seismic events can be detected.
4. *access:* Access tunnels and boreholes may limit the geometry of the seismic monitoring array, which may degrade the accuracy of the computed seismic parameters (e.g. source location accuracy).

However, by proper design of the seismic experiment unique information about the induced changes in the rock mass can be gathered remotely. Although the Mine-By experiment was performed to assess excavation-induced damage, similar techniques could also be used to assess the rock mass response in other nuclear-waste management applications: damage rehabilitation; heating in the emplacement stage; sealing; and long term performance monitoring.

ACKNOWLEDGEMENTS

The authors wish to thank AECL for its continued support of seismic research at the URL.

REFERENCES

[1] Read, R.S., and Martin, C.D..Monitoring the excavation-induced response of granite. In . of the 33rd US Symp. on Rock Mech. (Balkema, Rotterdam), 201-210, 1992

[2] Young, R.P., and Martin, C.D.. Potential role of acoustic emission/microseismic investigations in the site characterization and performance monitoring of nuclear waste repositories. Int. J. Rock Mech. Min. Sci. & Geomech. Abstr., 30, 797-803, 1993.

[3] Collins, D.C, and Young, R.P.. The spatial and temporal distribution of microseismicity recorded in round 17 of the Mine-by tunnel. Keele University Report to AECL, #RP023AECL, 1994.

[4] Gibowicz, S.J., Young, R.P., Talebi, S., Rawlence, D.J. Source parameters of seismic events at the Underground Research Laboratory in Manitoba, Canada: Scaling relations for events with moment magnitude smaller than -2. Bull. Seism. Soc. Am., 81, 1157-1182, 1991.